Journal of Alloys and Compounds 505 (2010) 634–639

Contents lists available at ScienceDirect

Journal of Alloys and Compounds

journal homepage: www.elsevier.com/locate/jallcom

Characterization and optical absorption studies of VO^{2+}:Li_2O–K_2O–Bi_2O_3–B_2O_3 glass system

M. Subhadra, P. Kistaiah*

Department of Physics, University College of Science, Osmania University, Hyderabad 500 007, India

ARTICLE INFO

Article history:
Received 9 April 2010
Received in revised form 10 June 2010
Accepted 12 June 2010
Available online 25 June 2010

Keywords:
Alkali bismuth borate glasses
Glass transition temperature
Optical absorption
Mixed alkali effect

ABSTRACT

Mixed alkali bismuth borate glasses xLi_2O–$(30-x)$ K_2O–$10Bi_2O_3$–55 B_2O_3 ($0<x<30$) doped with 5 mol% vanadium ions were prepared from the melts. These glasses were characterized using X-ray diffraction, differential scanning calorimetry and density measurements. Optical absorption studies were carried out as a function of alkali content to look for mixed alkali effect (MAE) on the spectral properties of these glasses. From the study of ultraviolet absorption edge, the optical band gap energies and Urbach energies were evaluated. The average electronic polarizability of the oxide ion, optical basicity and the interaction parameters were also evaluated for all the glasses. Many of these parameters vary non-linearly exhibiting a minima or maxima with increasing alkali concentration, indicating the mixed alkali effect. An attempt is made to interpret MAE in this glass system in terms of its glass structure.

1. Introduction

Glasses have many technological applications due to their electrical and optical properties. B_2O_3 is established as glass forming oxide whereas Bi_2O_3 and V_2O_5 are conditional glass formers. Vanadium doped glasses are known to exhibit semiconducting properties. Growing attention has been given in the last two decades to glasses containing Bi_2O_3 owing to their optical properties [1–6]. The properties of bismuth glasses were studied by many authors to explain its role in glass structure [7–10]. Borate glasses containing Bi_2O_3 posses a high refractive index, show large polarizability, and high optical basicity [11]. These glasses have potential applications in the field of glass ceramics, layers for optical and electronic devices, thermal and mechanical sensors, reflecting windows and superconducting materials [12]. The Bi^{3+} ion has small field strength so Bi_2O_3 cannot form glass by itself [13]. However, in the presence of B_2O_3 glass formation is possible. The large glass formation region in bismuth borate glasses has been attributed to the high polarizability of the Bi^{3+} cations. This property of Bi^{3+} ions also makes the glass suitable as non-linear optical/photonic material with high non-linear optical susceptibility [14].

Mixed alkali glasses are unique from the point of view that certain properties change much more than normally anticipated from what appears to be a structurally and compositionally simple substitution of one alkali oxide for another. Mixed alkali effect in different physical properties is observed in silica, borate and phosphate glasses [15–17]. When two types of alkali metal ions are introduced into a glassy network, a phenomenon known as mixed alkali effect (MAE) is observed. It represents the non-linear variations in many physical properties, when one type of alkali ion in an alkali glass is gradually replaced by another while total alkali content in the glass being constant [18,19].

Considerable amount of work have been reported on bismuth borate glasses [13,20,1,21], but in the presence of alkali oxides and transition metal oxides, studies related to spectroscopic properties have been carried out to a little extent. In view of the aforementioned aspects, xLi_2O–$(30-x)$ K_2O–$10Bi_2O_3$–$55B_2O_3$:$5V_2O_5$ ($0<x<30$ mol%) glasses have been prepared and studied their optical properties to explore the relationship between the structure of the glass and its macroscopic behaviour. Further, some physical parameters have also been evaluated and their variation as a function of composition has been taken into account to supplement the results of MAE in optical properties.

2. Experimental

2.1. Glass preparation

Glasses having composition xLi_2O–$(30-x)$ K_2O–$10Bi_2O_3$–$55B_2O_3$:$5V_2O_5$ (LK glasses) with $x=5$, 10, 15, 20, 25 mol%, were prepared by conventional melt quench method. Analytical grade reagents of Bi_2O_3, Li_2CO_3, K_2CO_3, H_3BO_3, and V_2O_5 were used as starting materials. Table 1 lists the batch composition (the starting mixture) in mol% of glasses studied in the present work. The chemicals were weighed accurately in an electronic balance mixed thoroughly and ground to a fine powder. The batches were then placed in porcelain crucibles and melted in a programmable electrical furnace. The melt was held at a temperature of 1000 °C for 1 h and was shaken frequently to ensure proper mixing and homogeneity. The melt was then quenched

* Corresponding author at: Department of Physics, University College of Science, OU Campus, Osmania University, Hyderabad 500 007, India. Fax: +91 40 27090020.
E-mail address: pkistaiah@yahoo.com (P. Kistaiah).

0925-8388/$ – see front matter © 2010 Elsevier B.V. All rights reserved.
doi:10.1016/j.jallcom.2010.06.097

Table 1
Glass composition of the samples in xLi_2O–$(30-x)$ K_2O–$10Bi_2O_3$–$55B_2O_3$:$5V_2O_5$ glass system.

Sl. no	Code	x (mol%)	Composition in mol%				
			Li_2O	K_2O	Bi_2O_3	B_2O_3	V_2O_5
1	LK-5	5	5	25	10	55	5
2	LK-10	10	10	20	10	55	5
3	LK-15	15	15	15	10	55	5
4	LK-20	20	20	10	10	55	5
5	LK-25	25	25	5	10	55	5

to room temperature in air by pouring it onto a polished steel plate and pressing with another steel plate. These glasses were then annealed at 300 °C to obtain strain free transparent glasses.

2.2. Glass characterization

The glass formation was confirmed by X-ray measurements using Philips X-ray diffractometer PW/1710 with Cu Kα radiation (λ = 1.5406 Å) powered at 40 kV and 30 mA.

By using the Archimedes principle, the glass densities have been determined with xylene as the immersion liquid on a single-pan electrical balance to the nearest 0.001 mg. The densities (D) were calculated by using the formula

$$D = \frac{a * 0.86}{a - b}\ \mathrm{g/cm^3} \quad (1)$$

where a is the weight of the sample measured in air; b is the weight of the sample measured in xylene and density of xylene at room temperature = 0.86 g/cm^3.

The molar volume (V_m) of each glass sample was calculated using the formula

$$V_m = \frac{\sum x_i M_i}{D}\ \mathrm{cm^3} \quad (2)$$

where x_i is the molar fraction and M_i is the molecular weight of the ith component.

From the density data oxygen packing density (OPD) was calculated using the formula [22]

$$\text{Oxygen packing density} = \left(\frac{D}{M}\right) \times \text{number of oxygen atoms per formula unit} \quad (3)$$

where M is the total molecular weight of the glass composition.

DSC is used to characterize the glasses. The glass transition temperature (T_g) was determined from differential scanning calorimetry (DSC) using DSC 821e METTLER TOLEDO model (TA Instruments). For this purpose the powdered glass sample was heated in an aluminum pan at a rate of 10 °C/min in the temperature range 30–600 °C using nitrogen as purge gas.

2.3. Optical measurements

The optical absorption spectra of these glasses were recorded in the UV region in order to measure the optical absorption edges by using a UV Elmer Lambda 700 spectrophotometer in the wavelength range 200–800 nm.

3. Results and discussion

3.1. XRD, DSC, density and molar volume

X-ray diffraction is a useful method to detect readily the presence of crystals in a glassy matrix if their dimensions are greater than typically 100 nm. The X-ray diffraction pattern of an amorphous material is distinctly different from that of crystalline material. The XRD patterns of the present glass system did not reveal any discrete or sharp peaks, but the characteristic broad humps of the amorphous materials. Fig. 1 shows the typical X-ray diffraction patterns for the glass system.

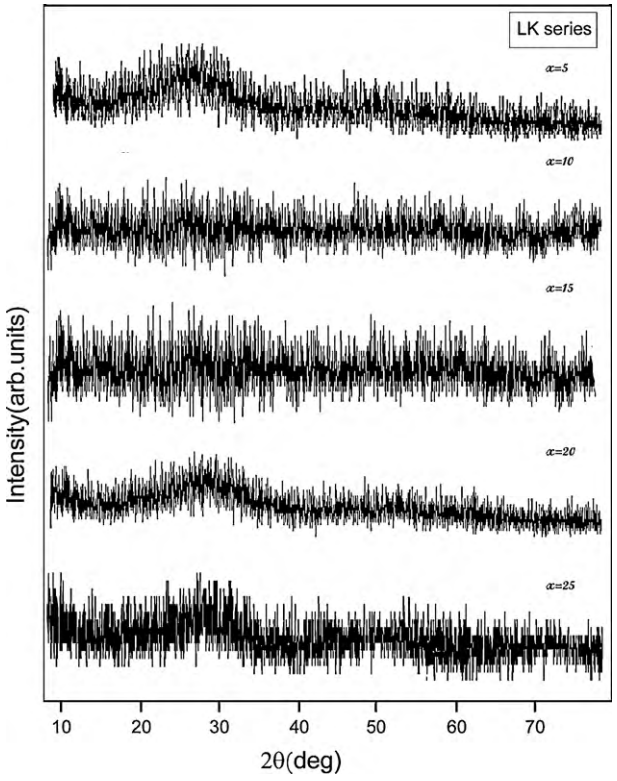

Fig. 1. X-ray diffraction patterns for different mixed alkali bismuth borate glasses: xLi_2O–$(30-x)$ K_2O–$10Bi_2O_3$–$55B_2O_3$–$5V_2O_5$ at room temperature.

The DSC pattern of LK-5 sample is shown in Fig. 2a. Fig. 2b shows the compositional dependence of glass transition temperature. In the present system all the glasses exhibit an endothermic peak due to the glass transition and the observed T_g lies in the range of 375–418 °C (Table 2). It is observed from Table 2 that glass transition temperature varies non-linearly with the concentration of Li_2O (x). The observed non-linear behaviour of glass transition temperature with x is a manifestation of mixed alkali effect in these glasses. The increase in the T_g is due to decrease in the number of non-bridging oxygen ions in the glass and is also associated with the formation of BO_4 tetrahedra which serve to cross-link the network by covalent B–O bonds. On the other hand the formation of borate network leads to a decrease in T_g. The non-linear variation of T_g with

Table 2
The density, molar volume, optical basicity, oxygen packing density, oxide ion polarizability, interaction parameter and glass transition temperature of the LK-series glass system.

Sample	Density (g/cm^3)	Molar volume (cm^3/mol)	Optical basicity (Λ_{th})	OPD (g-atm/l)	$\alpha_{O^{2-}}$ (E_o) (Å^3)	A	T_g (°C)
LK-5	3.27	36.43	0.688	68.63	3.25	0.0091	418
LK-10	3.30	35.08	0.680	71.26	3.16	0.0110	378
LK-15	3.36	33.47	0.672	74.68	3.04	0.0130	375
LK-20	3.43	31.84	0.664	76.88	2.98	0.0134	383
LK-25	3.43	30.94	0.656	80.8	2.91	0.0145	390

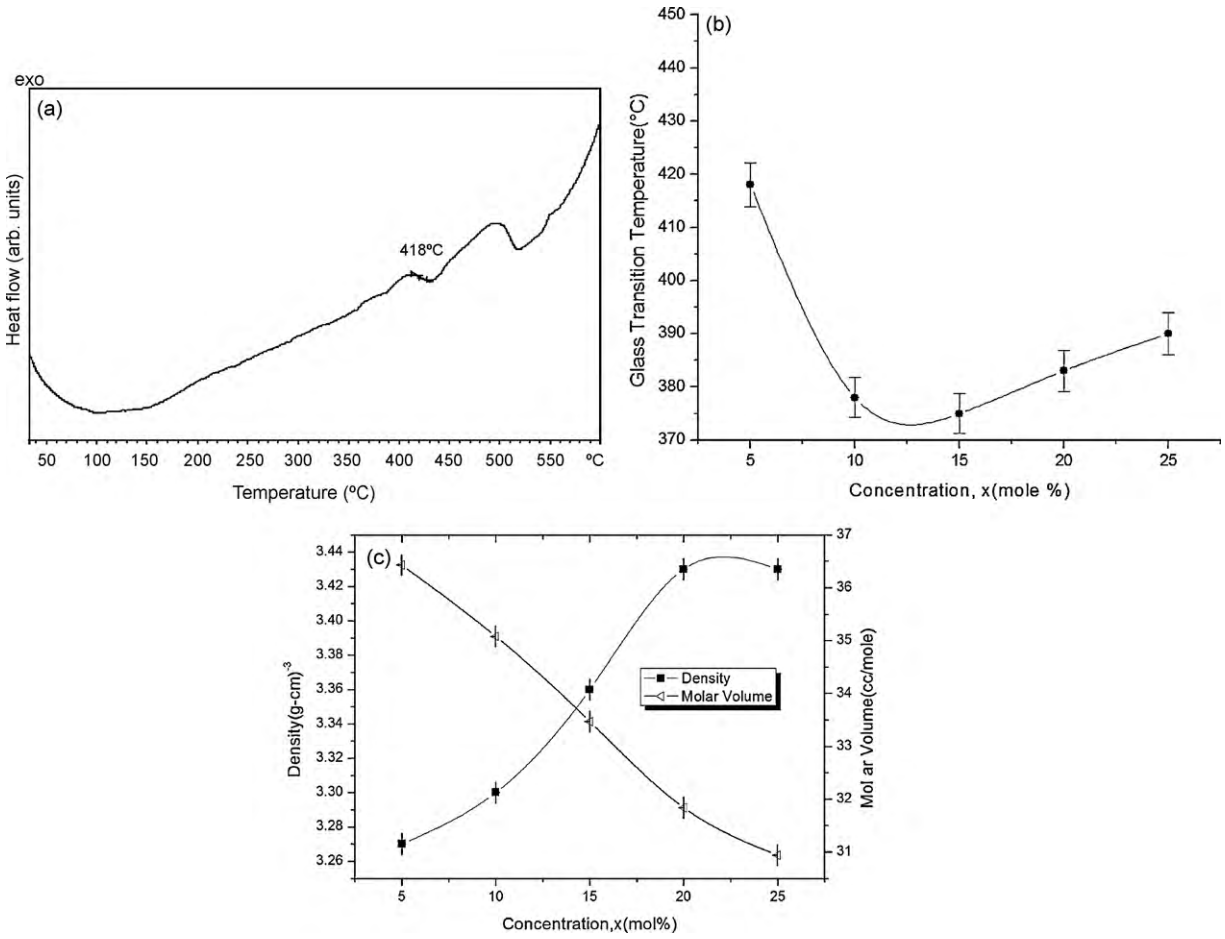

Fig. 2. (a) Typical DSC trace with heating rate of 10 °C/min showing the glass transition temperature (T_g) for LK-5 glass sample. (b) Compositional dependence of glass transition temperature of LK-series glasses. (c) Compositional dependence of density and molar volume of LK-series glasses.

(x) is due to the creation of BO_3 triangular (N_3), BO_4 tetrahedra (N_4), bridging and non-bridging oxygen ions.

The measured densities of the present glass system along with evaluated values of molar volume and oxygen packing density are also presented in Table 2. Fig. 2c shows the compositional dependence of density and molar volume. Density values are found to vary non-linearly with x depicting the mixed alkali effect. It is observed that the density increases continuously with increasing 'x' and after reaching a maxima at $x = 20$ it showed a small decrease when K_2O is replaced by Li_2O keeping Bi_2O_3 and V_2O_5 constant. The oxygen/boron ratio does not change in replacing one alkali oxide by another. Therefore, there would not be any significant change in the relative number of BO_3 units that convert into BO_4 units. This reveals that the increase in density may be due to contraction in the glass matrix when replacing the larger K^+ ions by smaller Li^+ ions. It is observed that molar volume decreases and oxygen packing density (OPD) increases continuously with increasing 'x' which may be due to decrease in non-bridging oxygen atoms.

3.2. Optical absorption studies

The study of optical absorption and particularly the absorption edge is a useful method for the investigation of optically induced transitions and for the provision of information about the band structure and energy gap in both crystalline and non-crystalline materials. The principle of this technique is that a photon with energy greater than the band gap energy will be absorbed.

Fig. 3a shows the optical absorption spectra of all the samples of LK-series glasses.

The absorption edge in many disordered materials follows the Urbach [23] rule given by

$$\alpha(\omega) = B \exp\left(\frac{\hbar\omega}{\Delta E}\right) \quad (4)$$

where $\alpha(\omega)$ is the absorption coefficient at an angular frequency of $\omega = 2\pi\nu$, B is the band tailoring parameter and ΔE is the width of the tail of localized states in the band gap (Urbach energy). At the absorption edge, random internal electric fields will dominate the broadening of the excitation levels due to the lack of long-range order or presence of defects [24].

There are two kinds of optical transitions at the fundamental edge of crystalline and non-crystalline semiconductors; direct transitions and indirect transitions, both of which involve the interaction of an electromagnetic wave with an electron in the valence band, which is then raised across the fundamental gap to the conduction band. For the direct optical transition from the valence band to the conduction band it is essential that the wave vector for the electron be unchanged. In the case of indirect transitions the interactions with lattice vibrations (phonons) take place, thus the wave vector of the electron can change in the optical transition and the momentum change will be taken or given up by phonons. In other words, if the minimum of the conduction band lies in a different part of k-space from the maximum of the valence band, a direct optical transition from the top of the valence band to the bottom of the conduction band is forbidden.

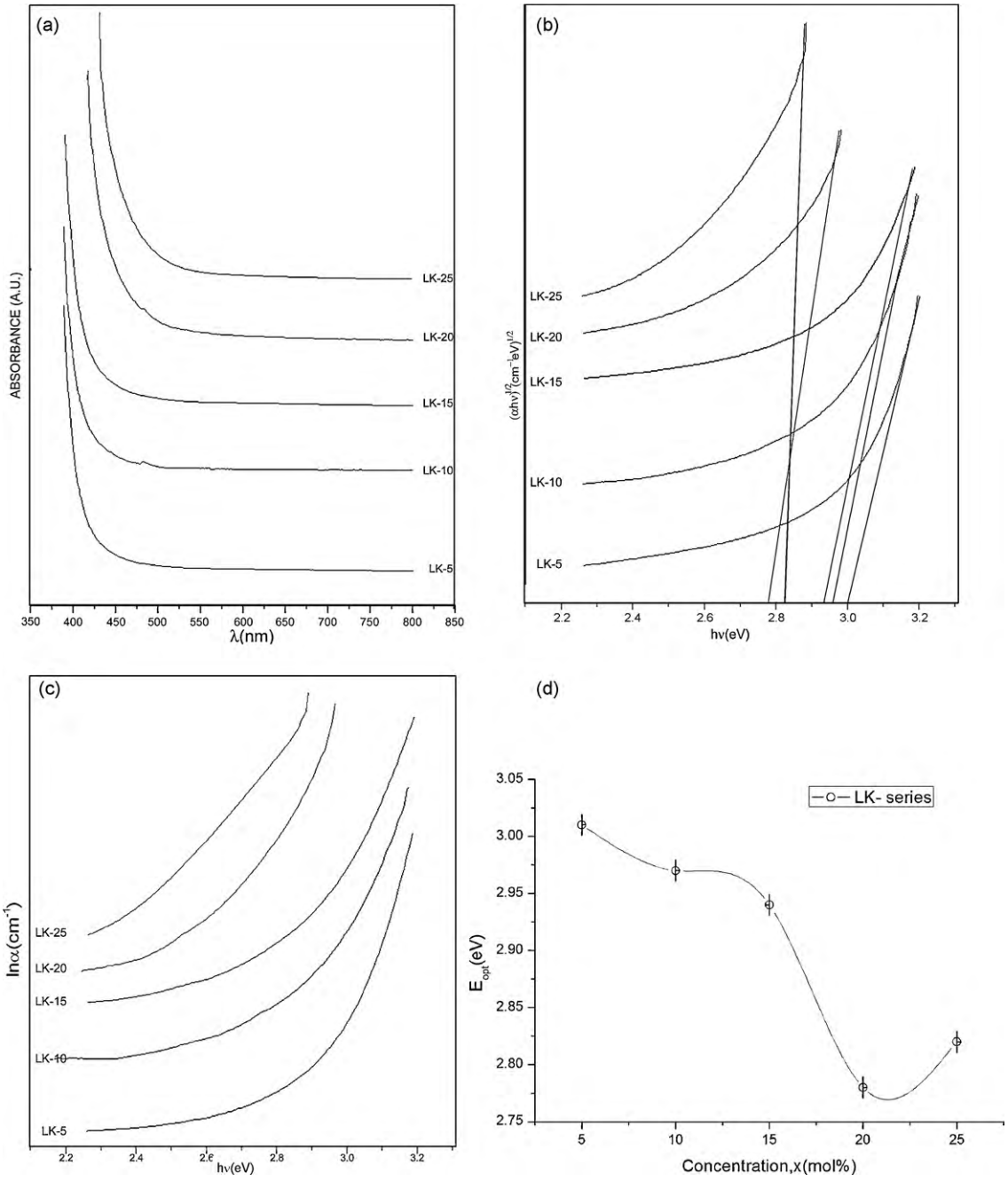

Fig. 3. (a) Absorbance vs. wavelength of LK-series glass system. (b) $(\alpha h\nu)^{1/2}$ vs. $h\nu$ of LK-series glass system (indirect transitions). (c) Urbach plots of LK-series glass system. (d) Variation of E_{opt} with Li_2O concentration.

The absorption coefficient $\alpha(\nu)$ can be determined near the edge using the formula:

$$\alpha(\nu) = \left(\frac{1}{d}\right) \ln\left(\frac{I_0}{I}\right) = 2.303\left(\frac{A}{d}\right) \quad (5)$$

where A is the absorbance at frequency ν and d is the thickness of the sample.

The absorption coefficient $\alpha(\nu)$ as a function of the photon energy $(h\nu)$ for direct and indirect optical transitions according to Mott and Davis [25] is given by

$$\alpha(\nu) = \frac{B(h\nu - E_{opt})^n}{h\nu} \quad (6)$$

where B is an energy-independent constant (band tailoring or band edge steepness parameter in Tauc's picture) [26] and the index n takes different values depending on the mechanism of interband transitions, i.e., $n = 2$ and 1/2 for indirect allowed transitions and direct allowed transitions.

For most of the amorphous materials indirect transitions are favored and according to Tauc's [26] picture, Eq. (6) for indirect allowed transitions changes to

$$E_{opt} = h\nu - \left(\frac{\alpha(\nu)h\nu}{B}\right)^{1/2} \quad (7)$$

The values of indirect optical band gap energy E_{opt} can be obtained from Eq. (7) by extrapolating the absorption coefficient to zero absorption in $(\alpha h\nu)^{1/2}$ vs. $h\nu$ plot and is shown in Fig. 3b. Plots were also drawn between $\ln\alpha$ and $h\nu$ (Fig. 3c) and from these plots, the slopes and thereby Urbach energies have been calculated.

Table 3
Cut off wave length, absorption edge, and optical energy gap of indirect transitions and Urbach energy of LK-series glass system.

SAMPLE	λ_c (nm)	Absorption edge (nm)	E_{opt} (indirect) (eV)	B (cm eV)$^{-1/2}$	Urbach energy (eV)
LK-5	390	413	3.01	90	0.166
LK-10	389	416	2.97	94	0.167
LK-15	390	406	2.94	102	0.165
LK-20	413	443	2.78	96	0.204
LK-25	430	452	2.82	103	0.210

The optical band gaps and Urbach energies obtained in the present work are given in Table 3.

From Table 3 it is observed that the optical band gap values for indirect transitions vary between 2.78 and 3.01 eV and they are inflecting with x. The non-linear variation of E_{opt} and also Urbach energy, ΔE with concentration (x) is an indication of the MAE in this glass system. Similar variations were observed in some mixed alkali borate glasses [27–29]. In the present glass system the absorption edges for different mol% of x are tabulated in Table 3. The variation of E_{opt} with concentration of Li_2O is shown in Fig. 3d. It is observed from Table 3 that there is a sharp decrease in edge shift for x = 15 mol% of glass and the edge shift thereafter increases for x = 20 and 25 mol%. As x increases from 5 to 15 mol% the cut off wavelength shifts towards shorter wavelengths whereas after that it shifts towards longer wavelengths.

3.3. Optical basicity and polarizability

The optical basicity of an oxide glass will reflect the ability of the glass to donate negative charge to the probe ion and is used as a measure of the acid–base properties of oxides [30,31]. The theoretical optical basicity (Λ_{th}) of multi-component glass can be obtained using the following equation proposed by Duffy and Ingram [32]:

$$(\Lambda_{th}) = X_1\Lambda_1 + X_2\Lambda_2 + \cdots + X_n\Lambda_n \quad (8)$$

where $X_1, X_2, \ldots, X_n$ are equivalent fractions based on the amount of oxygen each oxide contributes to the overall material stoichiometry and $\Lambda_1, \Lambda_2, \ldots, \Lambda_n$ are the basicities assigned to the individual oxides. Polarizability is one of the most important properties which govern the non-linear response of the material, since the optical non-linearity is caused by electronic polarization of the material upon exposure to intense light beams. Materials of higher optical non-linearity are designed on the basis of correlation of the optical non-linearity with some other electronic properties [33]. Therefore estimation of polarizability of glasses is useful owing to their technological importance as optical and electronic materials.

For ternary glasses with a general formula $X_1A_pO_qX_2B_rO_sX_3C_nO_m$ where X denotes the molar fraction for each oxide, the oxide ion polarizability is calculated using the following equation:

$$\alpha_{O^{2-}}(n) = \frac{\{(R_m/2.52) - \sum\alpha_{cat}\}}{N_{O^2}} \quad (9)$$

where $\sum\alpha_{cat}$ denotes molar cation polarizability given by $X_1p\alpha_A + X_2r\alpha_B + X_3n\alpha_C$ and $N_{O^{2-}}$ denotes the number of oxide ions in the chemical formula given by $X_1q + X_2s + X_3m$. The molar cation polarizability $\sum\alpha_{cat}$ of the glasses is calculated using the data on the polarizability of cations taken from the literature [34,35] and R_m is the molar refraction derived by Lorentz–Lorentz equation [36,37].

On the basis of refraction data, Duffy [38] has established that an intrinsic relationship exists between electronic polarizability of the oxide ions $\alpha_{O^{2-}}$ and optical basicity of the oxide medium (Λ) as given by

$$\Lambda = 1.67\left[1 - \left(\frac{1}{\alpha_{O^{2-}}}\right)\right] \quad (10)$$

Eq. (10) as shown by Dimitrov and Sakka [33] in the case of simple oxides facilitates the calculation of the optical basicity of the medium on the basis of experimental data for refractive index, n or for the energy gap E_{opt}. The optical basicity values of the individual oxides are taken from literature [33,34,39]. The optical basicity values of the glass samples were calculated and tabulated in Table 2 and are found to decrease with increasing Li_2O concentration.

Dimitrov and Sakka [33] proposed the following expressions for calculation of the electronic oxide ion polarizability of a simple oxide ($\alpha_{O^{2-}}$) on the basis of two independent initial values: linear refractive index (n_0) and energy gap (E_g):

$$\alpha_{O^{2-}}(n_0) = \left[\frac{(V_m/2.52)(n_0^2 - 1)}{(n_0^2 + 2) - p\alpha_i}\right] q^{-1} \quad (11)$$

$$\alpha_{O^{2-}}(E_g) = \left[\left(\frac{V_m}{2.52}\right)\left(1 - \frac{\sqrt{E_g}}{20}\right) - p\alpha_i\right] q^{-1} \quad (12)$$

The oxide ion polarizability values of the glass samples were calculated and tabulated in Table 2 and are found to decrease with increasing Li_2O concentration.

3.4. Interaction parameter

According to Yamashita and Kurosawa [40], the interaction parameter is a quantitative measure for the interionic interaction of negative ions such as F^- and O^{2-} with the nearest neighbors. It represents the charge overlapping of the negative ion with its nearest positive neighbour. It correlates with reducing the polarizability of negative ion placed in a crystal lattice in respect to the free-ion polarizability. Dikshit and Kumar based on the theory proposed by Yamashita and Kurosawa derived an expression for the calculation of the interaction parameter A for a given cation–anion pair [41]

$$A = \frac{(\alpha_f^+ + \alpha_f^-) - (\alpha_c^+ + \alpha_c^-)}{2(\alpha_f^+ + \alpha_f^-)(\alpha_c^+ + \alpha_c^-)} \quad (13)$$

where α_f^+ and α_f^- are the electronic polarizabilities of the positive and negative ions in free state while α_c^+ and α_c^- are the electronic polarizabilities of the ions in crystal under consideration. For metal (or nonmetal) – oxygen ionic pair, after substituting $\alpha_c^- = \alpha_{O^{2-}}$ and $\alpha_c^+ \approx \alpha_f^+$, we get

$$A = \frac{(\alpha_f^- - \alpha_{O^{2-}})}{2(\alpha_f^+ + \alpha_f^-)(\alpha_f^+ + \alpha_{O^{2-}})} \quad (14)$$

where now α_f^- is the electronic polarizability of free oxide ion and its value is 3.921 Å^3 and $\alpha_{O^{2-}}$ is its polarizability in the crystalline oxide under consideration. It has been established that the Yamashita–Kurosawa interaction parameter A is closely related to the oxide ion polarizability and optical basicity of oxide glasses. That is, the larger the oxide ion polarizability and optical basicity, the smaller is the interaction parameter. The values of interaction

parameter of the present glass system were calculated and tabulated in Table 2.

It is observed from the Table 2 that the value of optical basicity, oxide ion polarizability of the present samples decrease with increasing 'x' whereas the interaction parameter increases. It is understood from Eq. (14) that lower the oxide ion polarizability, greater is the interaction parameter. Since the oxide ion polarizability ($\alpha_{O^{2-}}$) depends on molar volume and molar volume is decreasing continuously, $\alpha_{O^{2-}}$ is also decreasing with the result optical basicity decreases and the interaction parameter increases.

4. Conclusions

The present study on multi-component bismuth borate glass system revealed the following conclusions:

- Multi-component glass system with composition, xLi$_2$O–$(30-x)$ K$_2$O–10Bi$_2$O$_3$–55B$_2$O$_3$ $(0<x<30)$ doped with 5 mol% of V$_2$O$_5$ is prepared through conventional melt quench technique.
- Amorphous nature of the samples is confirmed by the broad diffused haloes in XRD patterns.
- DSC measurements were carried out to determine the glass transition temperature (T_g) of the glass samples. T_g is found to decrease with the concentration of Li$_2$O depicting a minima at x = 15 mol% and thereafter increase for x = 20 and 25 mol% exhibiting MAE.
- The density of the samples is found to increase with the increase in the concentration (x), whereas the molar volume is found to decrease continuously owing to the contraction in the glass matrix due to replacing the larger K$^+$ ions by smaller Li$^+$ ions.
- Optical basicity and oxide ion polarizability are found to decrease with increasing concentration whereas interaction parameter is found to increase in accordance with the theory proposed by Dikshit and Kumar.
- From the optical absorption studies it is observed that the optical absorption edges are not sharply defined a characteristic of amorphous nature of samples.
- A shift towards longer wavelengths with increasing Li$_2$O concentration is observed in the cut off wavelength and absorption edge.
- Evaluated optical parameters like absorption edge, indirect optical band gap, band tailoring parameter B and Urbach energy showed non-linear variation with the Li$_2$O concentration manifesting the mixed alkali effect in this system.

Acknowledgements

One of the authors Mrs. M. Subhadra thanks UGC for financial assistance through Research Fellowships in Science for Meritorious Students (RFSMS) and the authors thank IICT, Hyderabad for providing experimental facilities. The authors also thank the reviewers for their critical comments and useful suggestions.

References

[1] W.H. Dumbaugh, Phys. Chem. Glasses 19 (1978) 121.
[2] W.H. Dumbaugh, Phys. Chem. Glasses 27 (1986) 119.
[3] V. Dimitrov, Y. Dimitrov, A. Montenero, J. Non-Cryst. Solids 180 (1994) 51.
[4] R. Iondanova, V. Dimitrov, Y. Dimitrov, D. Kissurski, J. Non-Cryst. Solids 180 (1994) 58.
[5] F. Miyaji, T. Yoko, J. Jin, S. Sakka, T. Fukanaga, M.J. Misawa, J. Non-Cryst. Solids 175 (1994) 211.
[6] M.M. Wierabicki, J.E. Shelby, Phys. Chem. Glasses 36 (1995) 150.
[7] J.T. Randall, H.P. Rooksby, J. Soc. Glass Tech. 30 (1933) 287.
[8] M.S.R. Heynes, H. Rawson, J. Soc. Glass Tech. 41 (1957) 347.
[9] Bh.V. Janakirama Rao, J. Am. Ceram. Soc. 45 (1962) 555.
[10] C. Hiryama, E.C. Subbarao, Phys. Chem. Glasses 3 (1962) 111.
[11] V. Dimitrov, T. Komatsu, J. Non-Cryst. Solids 249 (1999) 160.
[12] L. Baia, R. Stefen, W. Kiefer, J. Popp, S.J. Simon, J. Non-Cryst. Solids 303 (2002) 379.
[13] W.H. Dumbaugh, J.C. Lapp, J. Am. Ceram. Soc. 75 (1992) 2315.
[14] K. Terashima, T.H. Shimato, T. Yoko, Phys. Chem. Glasses 38 (1997) 211.
[15] R.M. Hakim, D.R. Uhlmann, Phys. Chem. Glasses 8 (1967) 174.
[16] H. Jain, H.L. Downing, N.L. Peterson, J. Non-Cryst. Solids 64 (1984) 335.
[17] H.M.J.M. vanAss, J.M. Stevels, J. Non-Crystal. Solids 15 (1974) 215.
[18] D.E. Day, J. Non-Cryst. Solids 21 (1976) 343.
[19] M.D. Ingram, Phys. Chem. Glasses 28 (1987) 215.
[20] T. Suzuki, M. Hirano, H. Hosono, J. Appl. Phys. 91 (2002) 4149.
[21] R. Nadjd-Sheibani, C.A. Hogarth, J. Mater. Sci. 26 (1991) 429.
[22] N.H. Ray, J. Non-Cryst. Solids 15 (1974) 423.
[23] F. Urbach, Phys. Rev. 92 (1953) 1324 [25].
[24] R.P. Sreekanth Chakradhar, et al., Mat. Res Bull. 40 (2005) 1028.
[25] N.F. Mott, E.A. Davis, Electronic Processes in Non-Crystalline Materials, 2nd edn., Oxford University Press, Oxford, 1979, p.273.
[26] J. Tauc, Amorphous and Liquid Semiconductor, Plenum, New York, 1974.
[27] A.A. Ahmed, A.F. Abhas, F.A. Mostafa, Phys. Chem. Glasses 24 (1983) 43–46.
[28] A. Agarwal, V.P. Seth, S. Sanghi, P. Gahlot, S. Khasa, Mater. Lett. 58 (2004) 694–698.
[29] G. Padmaja, P. Kistaiah, J. Phys. Chem. A 113 (2009) 2397–2404.
[30] J.A. Duffy, M.D. Ingram, J. Am. Chem. Soc. 93 (1971) 6448.
[31] J.A. Duffy, M.D. Ingram, J. Non-Cryst. Solids 21 (1976) 373.
[32] J.A. Duffy, M.D. Ingram, in: D. Uhlman, N. Kreidl (Eds.), Optical Properties of Glass, American Ceramic Society, Westerville, OH, 1991, p. 159.
[33] V. Dimitrov, S. Sakka, J. Appl. Phys. 79 (1996) 1736.
[34] V. Dimitrov, T. Komatsu, J. Ceram. Soc. Jpn. 107 (1999) 1012.
[35] J.A. Duffy, J. Non-Cryst. Solids 297 (2002) 275.
[36] E.A. Moelwyn-Hughes, Physical Chemistry, Pergamum, London, 1961.
[37] H. Rawson, Properties and Applications of Glass, Elsevier, Amsterdam, 1980, pp. 161–167.
[38] J.A. Duffy, Phys. Chem. Glasses 30 (1989) 1.
[39] A. Ghosh, Nakamura, et al. Secondary Steel Making Principles and Applications, vol. 21, CRC Press LLC (Appendix 2.4), 2001.
[40] J. Yamashita, T. Kurosawa, J. Phys. Soc. Jpn. 10 (1955) 610–633.
[41] U.C. Dikshit, M. Kumar, Phys. Stat. Sol. (b) 165 (1991) 599–610.